ORIGINAL RESEARCH

Autologous Fat Grafting Promotes Macrophage Infiltration to Increase Secretion of Growth Factors and Revascularization, Thereby Treating Diabetic Rat Skin Defect

Yu Wang
Hao Zhang
Min Zhou
Xinzeyu Yi
Ping Duan
Aixi Yu [ORCID]
Baiwen Qi

Department of Orthopaedic Trauma and Microsurgery, Wuhan University Zhongnan Hospital, Wuhan, Hubei 430071, People's Republic of China

Background: Diabetic skin defect is difficult to manage in surgical clinics, and there is still lack of effective treatments for diabetic skin defects. Currently, autologous fat grafting (AFG) is promising in the field of reconstructive surgery, while macrophage infiltration in autologous adipose tissue is considered vital for tissue regeneration. But AFG is rarely applied to the treatment of diabetic skin defects, and whether macrophage infiltration assists AFG to promote wound healing is still unknown.

Methods: Full-thickness skin defect diabetic rats were divided into 3 groups: control group, autologous fat grafting (AFG) group and AFG with macrophage depletion (AFG+MD) group. We examined the amount of macrophages in the wounds bed and the expression level of inflammatory factors IL-10, IL-6, TNF-α, and also growth factors PDGF-β, TGF-β, IGF-1 at the same time. The content of collagen-I and α-smooth muscle actin protein in the wounds were determined by Western blot analysis. Finally, the healing of the wounds was evaluated.

Results: The AFG group showing more rapid healing, secreting more growth factors and more obvious vascularization in the healing process, compared with the control group. But, the secretion of growth factors and the construction of extracellular matrix (ECM) in the wounds were limited when macrophages were depleted after AFG.

Conclusion: AFG promotes the infiltration of macrophages to improve the healing environment of diabetic wounds by increasing the secretion of growth factors and revascularization, which provides a potential method for the treatment of diabetic skin defects.

Keywords: diabetic skin defects, autologous fat grafting, wound healing, macrophage depletion

Introduction

Diabetic skin defects are common challenges in reconstructive surgery.[1] The repair of skin defects is a complex, highly regulated process consisting of four stages: early inflammatory stage, mid proliferative stage and late remodeling stage, which involve interactions between skin cells, immune cells and extracellular matrix (ECM).[2] The healing of skin defects is critical in maintaining the barrier function of skin and moderate the further deterioration of skin defects.[3] With multiple disease processes, the cascade of events involved in the healing of diabetic skin defects can be affected and leading to arresting in chronic inflammatory phase,

Correspondence: Aixi Yu; Baiwen Qi
Wuhan University Zhongnan Hospital,
169 East Lake Road, Wuchang District,
Wuhan, Hubei 430071, People's Republic
of China
Tel/Fax +86 67813120
Email yuaixi@whu.edu.cn;
wb002162@whu.edu.cn

further causing local ischemia, resulting in chronic, non-healing wounds that subject the patient to significant discomfort and distress while draining the medical system of an enormous amount of resources.[4–6] However, limited self-renewal ability of skin in severe chronic diabetic wounds necessitates the use of different skin grafting methods like full-thickness skin grafting including the whole dermis and epidermis.[7,8] As chronic diabetic wounds have more necrotic tissues and ischemia, patients usually need to suffer a long process of skin debridement and the skin cannot be directly grafted.[9] Except for the difficulty of flap transplantation which requiring experienced surgeons, diabetic patients are still at risk of failure due to vascular disease.[10] Besides that, skin substitutes have long been used in grafts for skin defects, but these biological engineered dressings are quite costly, representing a significant barrier to widespread adoption.[11]

Recent advances in tissue engineering approaches have provided promising treatment options to meet the challenges of impaired skin wound healing such as diabetic wounds.[12] There is an abundance of literature supporting the efficacy of fat grafting in plastic and reconstructive cases, such as burn and scarring area.[13,14] Adipose tissue is an abundant source of adipose-derived stem cells (ADSCs), which have shown an improved outcome in wound-healing studies.[15,16] ADSCs are pluripotent stem cells with the ability to differentiate into different lineages and to secrete various cytokines initiating tissue regeneration process.[17,18] Whereas fat transplantation for the treatment of diabetic skin defects rarely been evaluated, and its mechanism in treating chronic wounds is unclear.

It has been hypothesized that macrophage may have a positive effect on the survival and retention of fat grafts because of improved proliferation and differentiations of ADSCs, reduced inflammation, and improved vascularisation.[19] There is also increasing interest in a possible synergistic effect of macrophage infiltration and adipose grafting in aspect of healing potential, although the evidence for this is very limited.[20] Due to the ease of collection and affordable properties, adipose tissue is an attractive source and worthy of attention for clinical translation.[21] Therefore, in this study, we evaluate the evidence of AFG on eliminating chronic inflammation, promoting the secretion of growth factors and revascularization in diabetic skin defect rat models. At the same time, we constructed a macrophage depletion diabetic rat model to explore whether the recruitment of macrophages after AFG had an important impact on wound healing.

Materials and Methods
Animals and Skin Defect Model

All procedures were carried out in compliance with the guide for the care and use of laboratory animal resources and the national research council, and approved by the Animal Biosafety Level 3 Laboratory of Wuhan University Institutional Animal Care and Use Committee (2,019,201). 8 weeks of age, about 250 g SD rats were obtained at the Laboratory of Wuhan University Zhongnan Hospital and housed in a controlled environment (12 hours light/dark cycle at 21°C) with free access to water and standard chow diet. After 7 days of adjusting to the new environment, all rats received intraperitoneal injections of STZ (Streptozocin, Sigma, USA; 60 mg/kg), and then given free access to food and water.[22] The weight and blood glucose level of all animals were measured every day after STZ administration. The glycemia of rats was measured by a glucometer in venous blood samples collected via tail veins. The day of the surgery (about 7 days after STZ injection), blood glucose levels were again determined and only rats with blood glucose greater than 300 mg/dl (16.7 mmol/L) were considered diabetic and included for subsequent experiments. The back of the diabetic rats was shaved, and using 70% alcohol and iodophor disinfectant solutions to disinfect the skin surgery area of SD rats. After anesthesia with 1% pentobarbital sodium (40 mg/kg; i.p.), a 1.5×1.5 cm^2 full-thickness skin and subcutaneous panniculus carnosus were removed.[23]

Study Groups

Forty-five diabetic rats were divided into 3 groups randomly: the control (CON) group, the autologous fat grafting (AFG) group and the AFG with macrophage depletion (AFG+MD) group. The CON group rats were only covered with petrolatum gauze. For the AFG group rats, the autologous adipose tissues of rats inguinal regions were dissected using sterile surgical instruments, then rinsed with PBS (pH=7.4), minced with an ophthalmic scissors, and homogenized with PBS as well. The homogenized adipose tissue was then centrifuged in a test tube at 3,000 g for 3 minutes to remove water and oil.[24] The final products were transplanted to the skin defects. Likewise, the AFG wounds were covered with petrolatum gauze. Finally, for the AFG+MD group rats, before receiving AFG treatment, 100 μL Lipo-Clo (ClodronateLiposome, Netherlands; i.v.) was injected into rats using an insulin syringe every other day

for 2 weeks.[25] Every time the AFG+MD group rats injected with Lipo-Clo, the other two groups of rats would receive 100 μL of PBS solution as control.

Wound Closure Measurement

Gross wounds were observed and photographed at 0, 3, 5, 7, 10, and 14 days after the operation. The wound area was measured by a 15-centimeter sterile measuring ruler and also traced the wound margin on photograph and calculated the pixel data using ImageJ software (National Institutes of Health, Bethesda, USA).

Histology and Morphology Studies

Four rats from each group were sacrificed at day 7 and day 14 after surgery and the wound areas were excised for histological analysis. Sections of paraffin-embedded wounds were stained with Hematoxylin and Eosin (H&E) and were used to determine the thickness of granulation tissue and length of reepithelialization. The reepithelialization length was defined as the distance from the advancing tip of the epithelialization tongue to the site of the first hair follicle at the wound margin. Measurements were made using ImageJ software. Masson trichrome staining was performed on day 14 specimens to observe the collagen fibril alignments.

Immunohistochemistry for CD68 and CD31

CD68 was used to identify and quantify macrophages and the angiogenesis was measured with immunohistochemistry by CD31 assay on day 14 wound sections. Paraffin-embedded sections were rehydrated and subjected to antigen retrieval by microwaving in 10 mM sodium citrate (pH = 6.0) for 10 minutes. Immunohistochemistry was then performed using standard protocols as described before.[23] Primary antibodies used were as follows: anti-CD68 or anti-CD31 (Abcam, USA). Secondary antibody used was horseradish peroxidase-conjugated goat anti-rabbit IgG (Abcam). Primary antibodies were incubated at 4°C overnight and following secondary antibody labeling. Tissue sections were viewed using a Nikon ECLIPSE E600 microscope (Nikon, Japan).

Immunofluorescent Staining

Immunofluorescent staining was performed following previously described procedure[26] with the following primary antibodies: anti-CD68 (1:100; Abcam), anti-alpha smooth muscle actin (1:200; Abcam), anti-Collagen I (1:200; Abcam). The following secondary antibodies were used for double staining: Goat polyclonal secondary antibody to rabbit IgG (FITC; Abcam) and donkey anti-goat IgG (Cy5 ®; Abcam). Nuclei were stained with DAPI (Sigma-Aldrich, USA). The specimens were pretreated through heating followed by blocking with 1% BSA (Sigma-Aldrich) and then incubated with the primary antibody at 4°C overnight. After primary antibody staining, the specimens were washed with PBS, incubated with a secondary antibody, stained with DAPI and mounted on coverslips. Serial sections of the specimens were observed with a digital pathology scanner (APERIO VERSA 8; Leica).

Blood Vessel Density Quantitation

To quantify angiogenesis, blood vessel density of the wound beds on each tissue slides was determined. High-power (200×) images of CD31-stained sections were used for analysis. The neovascular area (CD31$^+$ cells) was measured using ImageJ and expressed as the percentage of CD31$^+$ area of the entire imaged area. Measurements were obtained using ImageJ software.

Quantitative Real-Time PCR Analysis

Skin samples including the wound and 4-mm margin of surrounding skin were harvested at day 3, 5, 7, and 14 post-surgery and were snap-frozen in liquid nitrogen, and stored at −80°C for further real-time reverse-transcriptase polymerase chain reaction (PCR) studies. RNA was extracted using TRIzol reagent (Life Technologies, USA). Real-time polymerase chain reaction was performed using the DyNAmo Flash SYBR Green qPCR Kit (Thermo Scientific, USA) on a real-time polymerase chain reaction detection system (Bio-Rad, USA). The primers designed for this study were shown in Table 1. The amount of each RNA sample was normalized to the housekeeping gene GAPDH. To compare across all experimental groups, we further normalized the results against the values from the control group. Relative gene expression quantification was calculated according to the comparative threshold cycle method ($2^{-\Delta\Delta Ct}$).

Western Blot Analysis

Total protein was extracted from the wound samples with RIPA (Beyotime, China) for at least 30 mins and the protein concentrations were determined using the BCA Protein Assay Kit (Beyotime) according to the manufacturer's protocol. 40 μg of total protein samples per group

Table 1 Custom Primer Sequences for Rat Gene Transcript Analyses

Genes	Forward	Reverse
GAPDH	TACTGTTGTCCAGCTACGGC	CGTCCAAATCCATTGATGCCC
CD68	CTGGACTCAGCAGCTCTACC	TTTCCCTGTTCCTTGGGCTAC
IL-6	ACCGCTATGAAGTTCCTCTCTGCAA	TGCAGGTTGCTCAAGCAGCA
IL-10	TCCGGGGTGACAATAACTGC	GACACCTTTGTCTTGGAGCTTA
TNF-α	TGATCCGAGATGTGGAACTGG	CTCCTCCGCTTGGTGGTTT
TGF-β	TACGCCAAAGAAGTCACCCG	GCCCTGTATTCCGTCTCCTTG
PDGF-β	CAAGACGCGTACAGAGGTGT	GTTTGAGGTGTCTTGGCTCG
IGF-1	GACCCGGGACGTACCAAAAT	TAGCCTGTGGGCTTGTTGAA
bFGF	AAGCGGCTCTACTGCAAGAA	GCTGTAGTTTGACGTGTGGG
FGF7	GCTTCCACCTCGTCTGTCTTGT	CCACAATTCCAACTGCCACA

was heated with SDS-PAGE sample buffer and separated on a 12% SDS-PAGE gel. Proteins were then transferred to a PVDF membrane in transfer buffer, and blocked for 1.5 h in 5% skim milk in TBST. The membranes containing the transferred proteins were incubated overnight at 4°C with primary antibodies against α-smooth muscle actin (α-SMA), collagen-I (Col-Iα) or GAPDH (Abcam, UK; 1:1000). Next, membranes were washed in TBS washing buffer and incubated with peroxidase-conjugated secondary antibodies.

Statistical Analysis

All values were expressed as means ± SD. For data comparisons, two-tailed *t*-test assuming equal variance was used. The nonparametric Mann–Whitney test was used for statistical analysis of quantitative reverse transcription polymerase chain reaction data. Statistical significance was set at * P < 0.05, ** P < 0.01, *** P < 0.001.

Results
Blood Glucose Level and Body Weight of Diabetic Rats

Diabetic SD rats in each group exhibited an average blood glucose level of 341.3 ± 9.59 mg/dL, and these levels were 2.8-fold higher than those observed in 8-week-old nondiabetic rats (121.3 ± 3.88 mg/dL). Diabetic SD rats exhibited an average body weight of 373.1 ± 5.79 g and these body weights were 1.5-fold higher than nondiabetic rats (242.0 ± 4.63 g). The above results are shown in Figure S1.

Depletion of Macrophages in Diabetic Rats

To analyze the functional impact of macrophages during diverse phases of skin repair, we established a macrophage depletion skin defects rat model (see material and methods section). First, we used qPCR to detect the changes in gene expression of CD68 in the wound margins on day 3, 5, 7 and 14 post surgery. The results showed that the expression of CD68 in wound margins increased with time, CD68 was rarely expressed in the CON group, and the expression of CD68 in the AFG group was significantly higher (* P < 0.05) than that in the AFG+MD group and the CON group as well at day 14 post surgery (Figure 1A). The qPCR results suggested that AFG could efficiently promote the infiltration of macrophages, but Lipo-Clo treatment depleted macrophages (by about 4-fold) at day 14 post-grafting (*P < 0.05). Then, we performed an anti-CD68 immunohistochemistry assay on day 14 wound sections and CD68-positive areas were quantified using ImageJ. The results showed that the CD68+ cells mostly exhibited in AFG group and those cells mainly clustered around the transplanted adipose tissue (Figure 1B). Further anti-CD68 immunofluorescence assessment of the survived adipose tissue from transplantation confirmed that macrophages (CD68+; red) mainly infiltrated around transplanted adipose tissue, and the content of macrophages in the AFG+MD group decreased significantly compared with AFG group (Figure 1C; white arrow shows the fat droplets).

Wound Closure

Digital photographs of wound areas were obtained at 0, 3, 7, 10, and 14 days after surgery (Figure 2A). Figure 2B intuitively showed the healing of all three groups of wounds at different time points. As revealed by the macroscopic analysis of wound closure (Figure 2C and D), depletion of macrophages (AFG+MD group) during the early inflammatory phase (Figure 2D; Day 0–3) resulted in significant delay of the early repair response compared
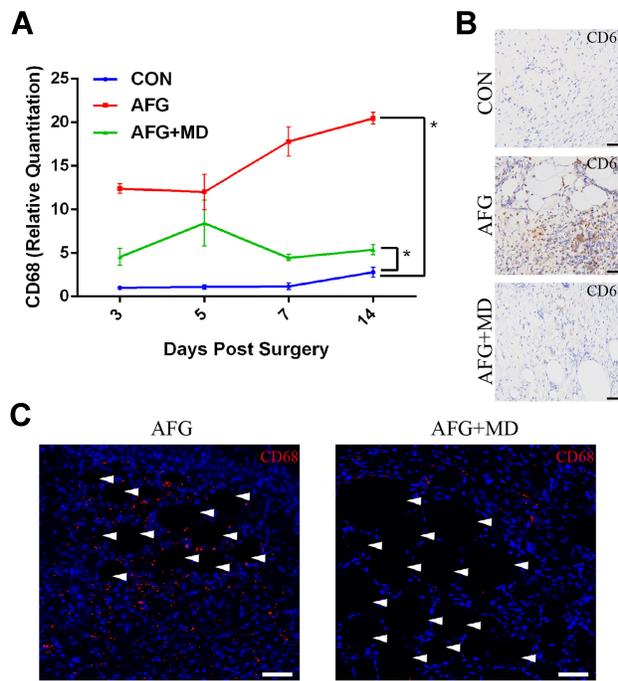
A

B

C

AFG   AFG+MD

Figure 1 The distribution and content of CD68-positive macrophages in diabetic wounds. (**A**) The relative quantitation of CD68 mRNA expression. (**B**) Anti-CD68 immunohistochemistry images of wound beds at day 14. Scale bar = 50 μm. (**C**) Anti-CD68 immunofluorescent assays for the survived adipose tissue of AFG or AFG+MD rats at day 14 post surgery (the white arrowhead shows the lipid droplets of adipose tissue). Scale bar = 50 μm. * P<0.05.

with AFG group (* P < 0.05). Whereas at day 7 post-surgery the wound area was reduced to 54.4% of the original wound size in AFG group. Meanwhile, the wound size of AFG+MD group rats was reduced by only 27.2%, and 29.3% in CON group (Figure 2D; Day 7). However, at the late stage of wound healing, all three groups showed almost the same healing rate (Figure 2D; Day 10–14). This validated that AFG can accelerate the healing of diabetic wounds compared with the CON group, however, depleted the macrophages (AFG+MD group) in the adipose tissue will delay the healing of the skin defect after AFG. Figure 2E demonstrates the distinct stages of skin repair response.

Histology

Above macroscopic findings were further confirmed by histological assessment. The sagittal sections of H&E–stained specimens collected on 7 days and 14 days post-surgery were presented in low-magnification microphotographs (Figure 3A). On Day 7, granulation tissue (g) was abundant in the AFG group (Figure 3A, b1), and neo-epithelial tongue (et) could be observed. However, the

CON group had less granulation tissue (g) content, and no obvious re-epithelialization (Figure 3A, a1). Comparing the AFG+MD group with AFG group on day 7, granulation tissue formation was noticeably reduced in the AFG +MD group and there was also no obvious epithelial tongue observed in AFG+MD wounds as well (Figure 3A, c1). Furthermore, we measured the thickness of granulation tissue by ImageJ to indirectly reflect the differences in the content of granulation tissue of day 7 wounds, and the measurement results were shown to be significant (* P < 0.05) between the AFG wounds and the other groups (Figure 3B). On the tissue images of day 14 wounds (Figure 3A; Day 14), a black fold line (shows the distance from the advancing tip of the epithelialization tongue to the site of the first hair follicle) was used to indicate the length of re-epithelialized epithelial tongue (et). The AFG group (950.4 ± 30.02 pixels) had significantly longer (* P < 0.05) et than that of the CON group (684.8 ± 49.27 pixels) and the AFG+MD group (576.4 ± 35.99 pixels) as well, the quantitative statistics of et measured by ImageJ are shown in Figure 3C. Moreover, incompletely formed skin appendages were seen in AFG specimen (Figure 3A, b2; red arrowhead shows), which was essential for restoring skin function. Whereas, fibrotic and dense scar tissue was seen in the CON wounds on day 14 post surgery (Figure 3A, a2), with no skin appendages observed. It could be seen that 14 days after surgery, the AFG+MD wounds had less extracellular matrix formation, indicating poor wound healing (Figure 3A, c2). The local magnified images (by 40× magnification) of day 14 wounds showed the proliferating keratinocytes.

The Expression of Inflammatory Factors and Wound Healing Related Growth Factors

We tested the expression of inflammatory factor IL-10, IL-6 and TNF-α in all three groups. As demonstrated in Figure 4A, the expression of IL-10 was not statistically significant (P > 0.05) between the three groups. The expression of IL-6 in the AFG group was less (* P < 0.05) than the other two groups in both early stage (Day 3) and late stage (Day 14) of wound healing. Compared with the CON group or AFG +MD group, AFG wounds expressed fewer (* P < 0.05) inflammatory factor TNF-α on day 14.

AFG were associated with a significantly higher mRNA expression level of growth factors PDGF-β and IGF-1 (*P < 0.05) when compared with the CON group
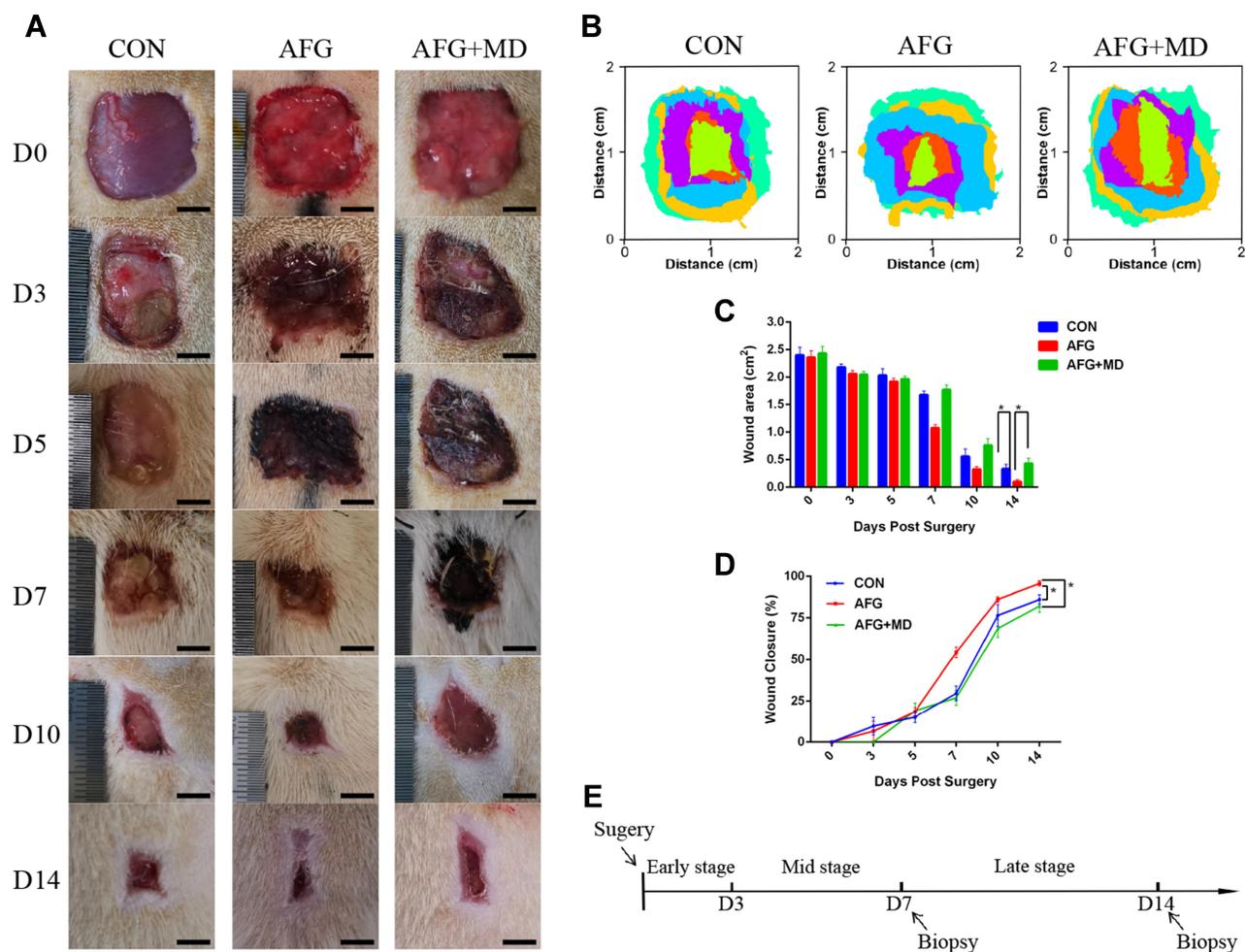
Figure 2 Gross wound appearance presentation and analysis. (**A**) Digital images of representative wounds images at day 0, 3, 5, 7, 10, 14. Scale bar = 0.5 cm. (**B**) ImageJ software used to reappear wounds healing process. Scale bar = 2 cm. (**C**) Quantification of the wound area. (**D**) The percentage of wound closure are presented by a fold line diagram. (**E**) Schematic representation of distinct stages during the skin repair response. *P<0.05.

and AFG+MD group through all stages of wound healing (Figure 4B). The secretion of TGF-β in AFG group mainly increased (* P < 0.05) on day 7 compared with other groups. These results confirmed that AFG benefited the secretion of growth factors at the time of transplantation, and macrophage depletion hindered the ability of AFG wounds to secrete growth factors.

Immunohistochemistry, Manson Trichrome Staining, Western Blot and qPCR for the Determine of ECM Formation

Blood vessels were identified 14 days after surgery using CD31 immunohistochemical staining (Figure 5A) and the CD31 positive microvessels were stained in brown. The blood vessel density was quantified by ImageJ, and as

shown in Figure 5B the vessel density increased in the AFG group compared with the CON group and AFG+MD group after 14 days (* P < 0.05). Macrophage depletion significantly affected the formation of new blood vessels in the wound after adipose tissue transplantation. We investigated proteins that involved in collagen formation and ECM formation. Showen by Figure 5D, the expression of α-SMA and Col-Iα protein in the AFG+MD wounds was significantly lower (*** P < 0.001) than those in the AFG group (the analysis results of Western blot displayed in Figure S2). In addition, Manson trichrome staining was subjected to evaluate the collagen alignment of wound bed (Figure 5C). There was an irregular and dense arrangement of collagen bundles in the CON group, suggesting scar formation. Whereas, the collagen fibril of AFG wound bed arranged neatly and uniformly. And the AFG+MD
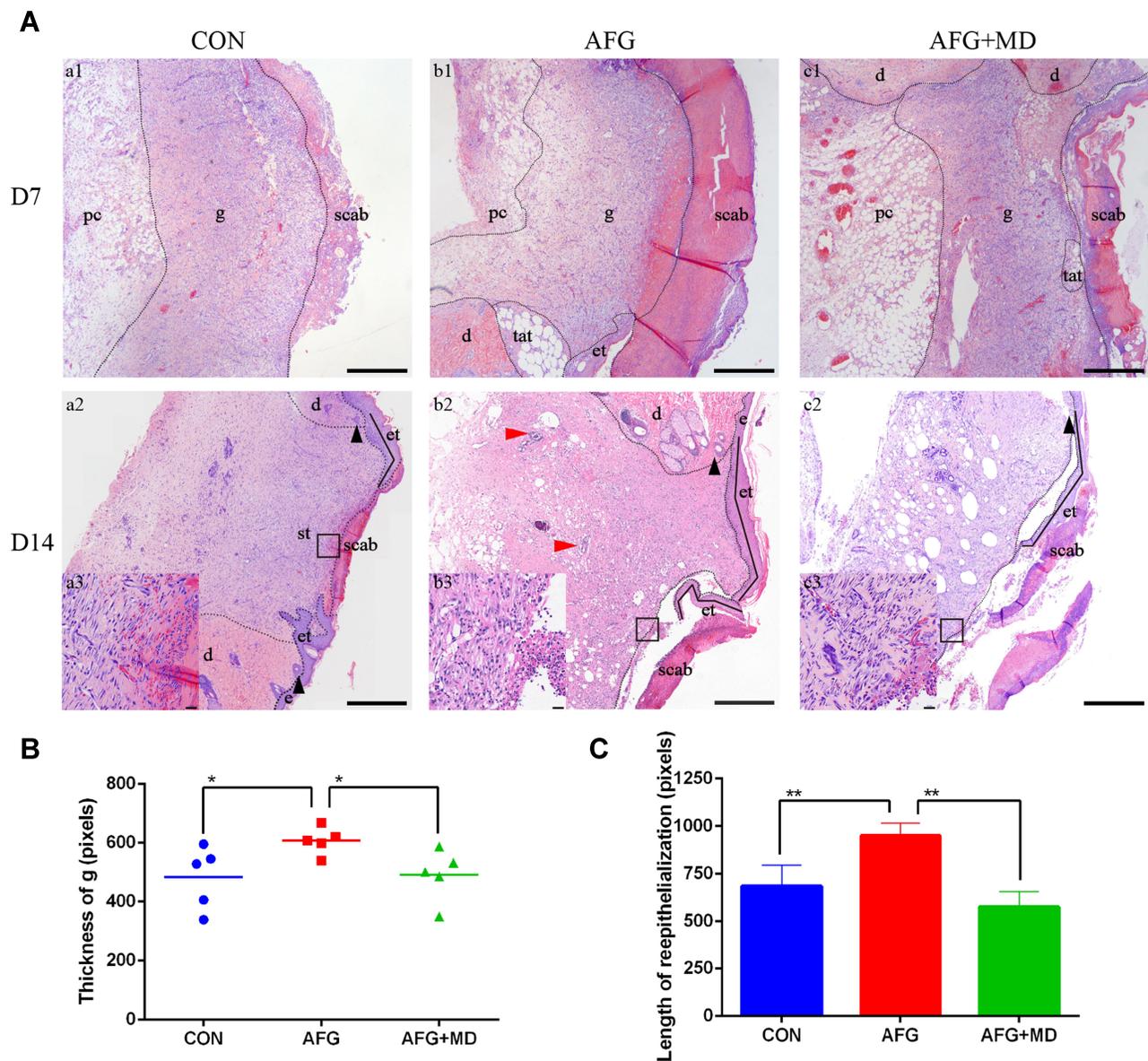
Figure 3 Histology and morphology studies of wounds. (**A**) H&E staining (40×magnification, scale bar = 200 μm) of wounds specimens at 7 and 14 days post surgery. Black dashed line outlines granulation tissue; black arrowhead shows the first hair follicle from wounds edge; black folded a black fold line shows the distance from the advancing tip of the epithelialization tongue to the site of the first hair follicle; red arrowhead shows incompletely formed skin appendages. (**B**) The thickness analysis of granulation tissue (g) of day 7 H&E stained wound sections by ImageJ. (**C**) The length analysis of reepithelialization of day 14 H&E stained wound sections by ImageJ. *P<0.05, **P<0.01.
Abbreviations: g, granulation tissue; e, epidermis; et, epithelial tongue; d, dermis; st, scar tissue; pc, panniculus carnosus.

wound showed an impaired collagen formation with reduction in ECM. Therefore, it could be considered that macrophage depletion hindered wound vascularization and the formation and remodeling of ECM.

As shown in Figure 5E and F, the wounds of the AFG +MD group secreted less fibroblast growth factors bFGF and FGF-7 (* P<0.05) than AFG and CON group. Previous studies had shown that bFGF and FGF-7 to be important during the later stages of neovascularization when luminal spaces and basement membranes are being

developed,[37] which was also critical for stabilization of ECM. These results also explained the poor vascularization and ECM formation of the AFG+MD group in the late stage of wound healing.

Immunofluorescence Staining for the Evaluation of AFG Treating Effect

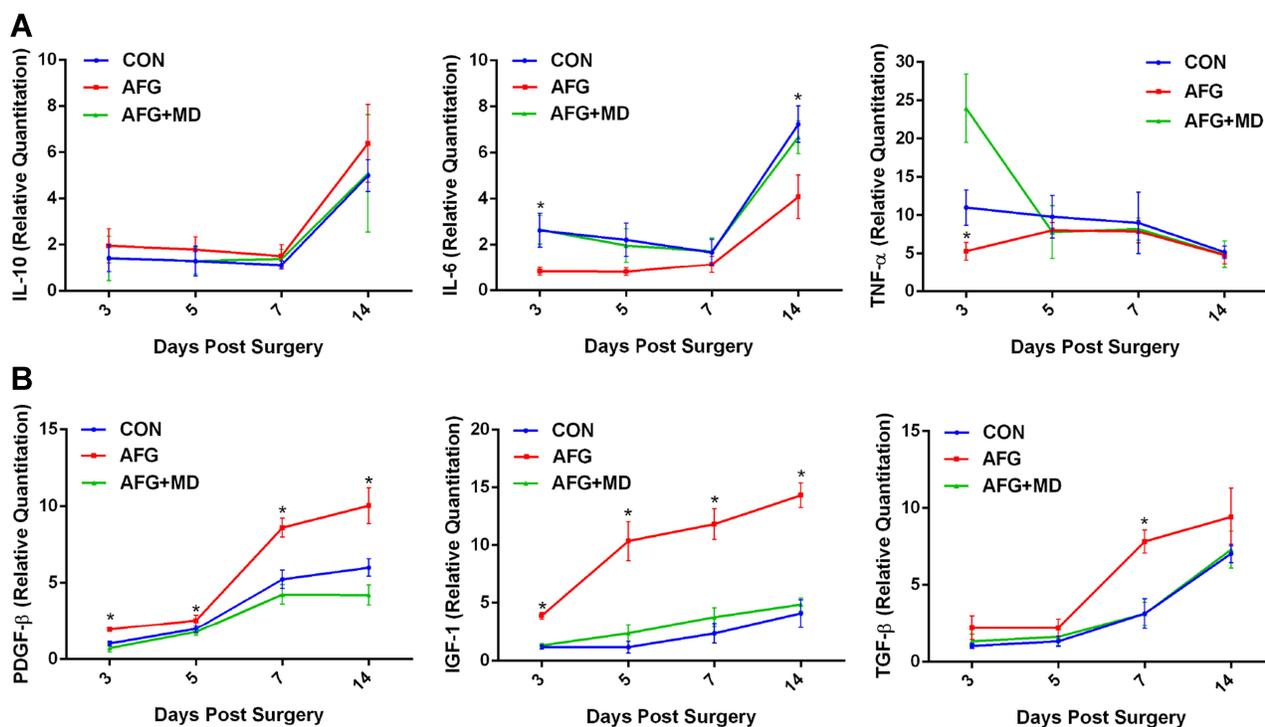To investigate the treating effect of AFG, we performed immunofluorescent double labeling for CD68 and α-SMA

Figure 4 The relative quantitation for mRNA expression of inflammatory factors and wound healing related growth factors. (**A**) The mRNA expression of inflammatory factor IL-10, IL-6 and TNF-α. (**B**) The mRNA expression of growth factor PDGF-β, IGF-1, TGF-β. *P<0.05 (the AFG group versus the CON group or the AFG+MD group).

or Col-Iα (Figure 6). At day 7 post surgery, α-SMA (green), the signature mediator for myofibroblast differentiation, was abundantly expressed throughout the entire layer of the granulation tissue, especially in neovascular endothelium in AFG wounds, along with CD68 (red) labeled macrophages (Figure 6A; AFG). In contrast, wounds of CON group showed weak α-SMA staining in the scarce granulation tissue at 7 d following surgery, and less expression of CD68 (Figure 6A; CON). The double staining of CD68 (red) and Col-Iα (green) showed that the CON wound presenting collagen aggregation on day 7 post surgery leading to early scar formation (Figure 6B; CON). In the AFG group, Col-Iα (green) were evenly distributed throughout the wound bed, resulting in an improvement of skin reconstruction quality.

Discussion

The healing of diabetic skin defects is delayed due to the imbalance of molecular interactions and cellular signal transduction, showing protracted inflammation, impaired angiogenesis and reduced growth factor levels.[27,28] The reduction of new blood vessels and the persistence of chronic inflammation in diabetic skin defects affect the time and quality of wound healing. It can even develop

into chronic non-healing wounds, causing a huge burden on the medical system.[19,29]

AFG is becoming a common procedure in face and body lipofilling surgeries, because of its high content of ADSCs and regeneration ability.[30,31] Adipose tissue also has the characteristics of ease to harvest, biosafety and affordable, therefore AFG is considering an ideal strategy for reconstruction surgery.[32,33] The adipose tissue contains various high-concentration growth factors, and those growth factors can cooperate with each other to expand the biological effect.[34] Such growth factors include platelet-derived growth factor-β (PDGF-β), Insulin-like growth factor-1 (IGF-1) and transforming growth factor-β (TGF-β), which can not only regulate cell migration and proliferation, but also transform the extracellular matrix (ECM) and promote angiogenesis to create a favorable environment for wound healing.[35–37] Another study showed that monocytes begin migrating into the wound and then differentiate into wound associated macrophages in the process driven by factors in the extracellular milieu.[38] And the high content of macrophages found in transplanted adipose tissue has the potential to promote ADSCs to differentiate into a wide range of regenerated tissue cells as well as improving proangiogenic qualities.[39] Based on
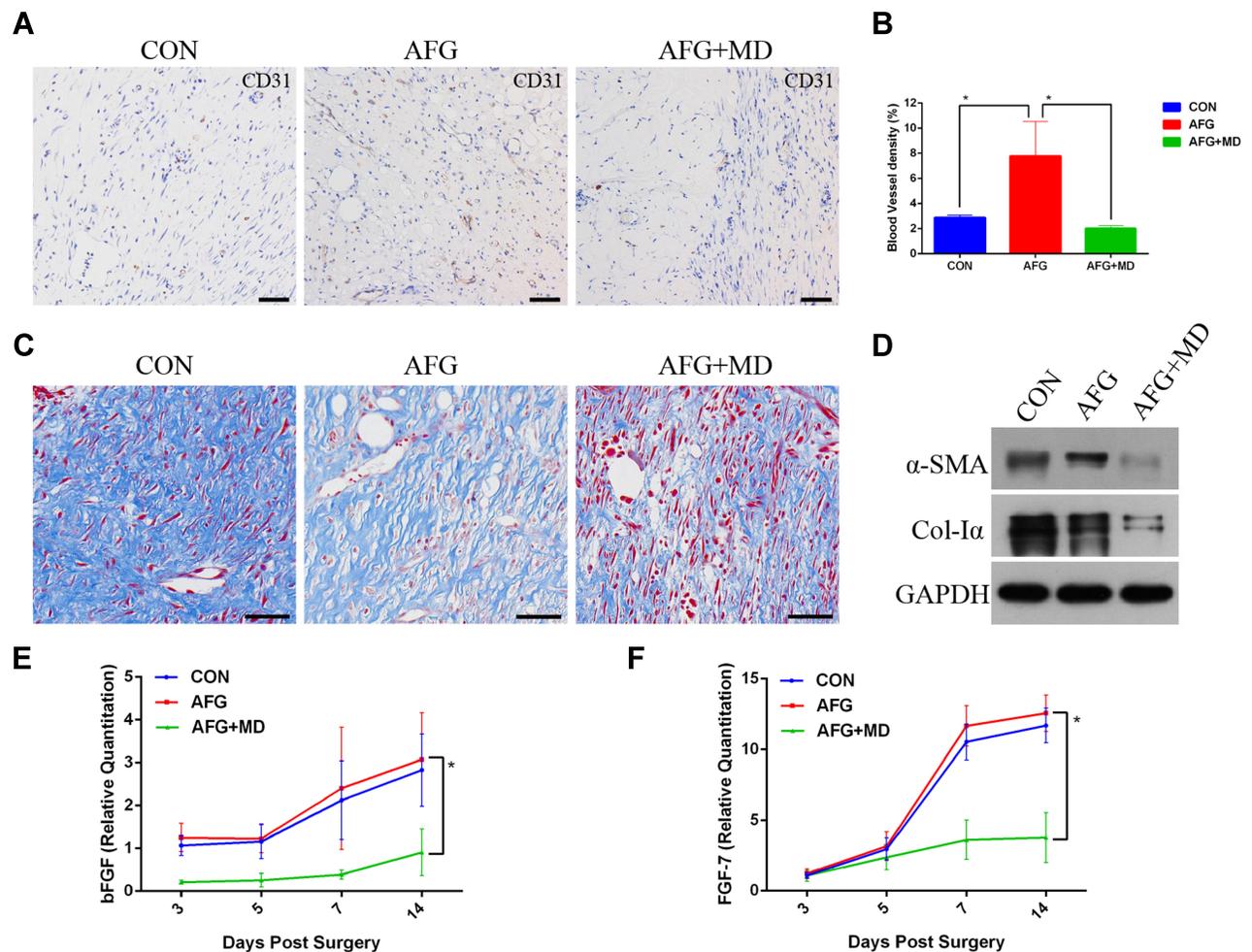
Figure 5 The analysis of ECM formation on day 14. (**A**) Anti-CD31 immunohistochemistry assays. Scale bar = 50 μm. (**B**) Quantification of blood vessel density by measuring the percentage of CD31-positive area. (**C**) Masson trichrome staining of day 14 wounds to evaluate the collagen formation. Scale bar = 50 μm. (**D**) Western blot assays of Col-Iα, α-SMA and GAPDH as an internal reference. (**E**) The relative quantitation of bFGF mRNA expression. (**F**) The relative quantitation of FGF-7 mRNA expression. *P<0.05.

the previous researches, we assumed that AFG may have the ability to impede chronic inflammatory response of diabetic wounds, promote vascularization and achieve skin defects reparation, and macrophage infiltration may play an important role in coordination with the AFG in wound-healing process.

In our study, we demonstrated the potential use of autologous fat grafting in the field of skin defect treatments. Although autologous fat grafting was widely used in clinical, its optimal application in soft-tissue treatments was still being explored. In the present study, the AFG group showed better and stronger healing of the wounds compared with the control group, this result was consistent with the previously reported results of using ADSCs to treat wounds.[40] We analyzed the wound closure percentage, re-epithelization length,

granulation tissue thickness and blood vessel density on day 14 wounds in order to evaluate the function of AFG to promote wound healing. The results revealed that AGF had the potential to settle the lack of growth factors and hypo-vascularization of diabetic skin defects. Also, the macrophage depletion hindered the AFG treatment effect by extending the wound-healing time. Furthermore, our CD68-labeled immunohistochemistry and immunofluorescence assessments results suggested that macrophages mainly infiltrate around the adipose tissue that survived after AFG, this finding suggested the possibility of a complementary effect of the AFG treatment and macrophages in treating diabetic skin defects. Our results showed that the expression of inflammatory factors in the AFG+MD group was lower than the AFG group, which revealed that macrophage depletion
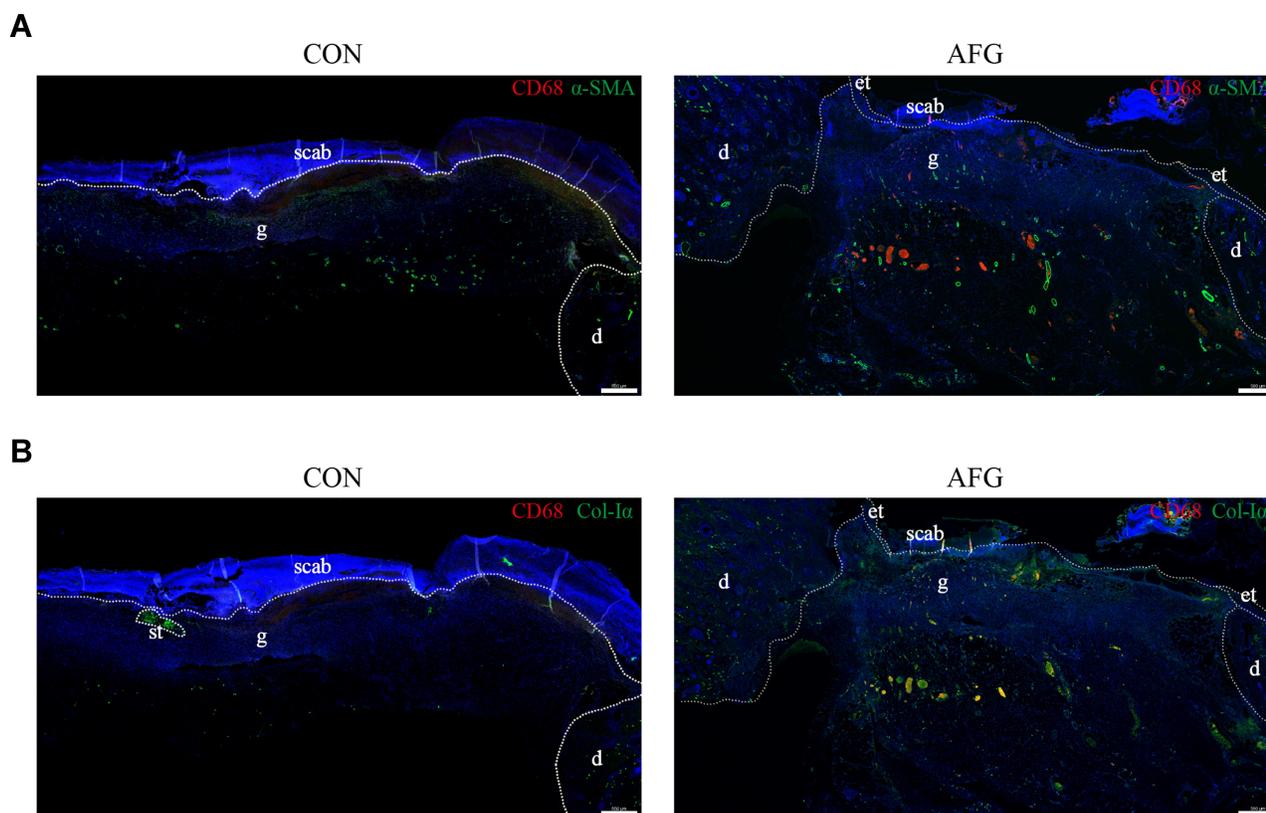
Figure 6 Immunofluorescent double-staining analysis. (**A**) Immunofluorescent double labeling for CD68 (red) and α-SMA (green). Scale bar = 200 μm. (**B**) Immunofluorescent double labeling for CD68 (red) and Col-Iα (green). The white dotted circle shows the scar tissue on the CON group. Scale bar = 200 μm.
Abbreviations: g, granulation tissue; e, epidermis; et, epithelial tongue; d, dermis; st, scar tissue; pc, panniculus carnosus.

after AFG could not achieve the effect of reducing inflammatory responses. By decreasing the expression of wound healing related growth factors, the wound microenvironment deteriorates functionally after macrophage depletion.

We have also found that AFG and macrophage infiltration were crucial for stabilization of vascular structures using anti-CD31 immunohistochemistry assays. The fat grafted rats expressed significantly elevated levels of CD31 expression, indicating greater vascularity compared with non-grafted rats. Subsequently, we further evaluated the CD31 expression on the AFG+MD rats, the results showed that the macrophage depletion significantly hindered the promoting effect of AFG to wound neovascularization.

Macrophages present at the late stage of the repair response impact tissue maturation and ECM formation. Collagens are the most abundant proteins in animals and constitute the main structural element of ECM.[41] In the granulation tissue, fibroblasts are activated and acquire α-SMA expression and become myofibroblasts.[42] These myofibroblastic cells synthesize and deposit the ECM components that eventually replace the provisional matrix.[43] As demonstrated in our study, the expression of Col-I and α-SMA dropped sharply in the AFG+MD group wounds comparing with the normal non-MD rats, suggesting a poor ECM formation and malunion of wound healing. Besides, in AFG+MD rat wounds, the expression of fibroblast growth factors bFGF and FGF-7 was restrained as well, resulting in a morphological change of the content of ECM decreased while the content of adipose tissue increased. Therefore, our studies provide evidence that macrophages cooperate synergistically with AFG treatment during wound repair response and they orchestrate the natural sequence of repair phases in skin, which are essential to restore solid tissue homeostasis and integrity postinjury.

Overall, our study adds to previous knowledge on the AFG can help tissue regeneration, but also uncovers several novel aspects. Firstly, for the first time, we verified that AFG can improve the lack of growth factors and ischemia of diabetic wounds, thereby promoting the healing of diabetic wounds and realizing functional wound

healing. Secondly, through pathological examination of the wounds, we found that macrophages mainly aggregated around the adipose tissue survived after AFG. Finally, we believe that macrophage infiltration is an important factor affecting wound healing, and likely to be a key factor for AFG treatment to achieve functional wound healing with relatively quick wound-healing time compared with standard wound management options. However, the process of wound healing and the mechanisms by which macrophages affect wound healing are very complicated. In order to explore the specific mechanism of the co-regulation of AFG and macrophages in the treatment of diabetic skin defects, further experimental studies are quite required.

Conclusion

This study demonstrates that AFG can improve ischemia of diabetic wounds and secrete growth factors to promote re-epithelialization and revascularization of wounds, which brings a new hope for the treatment of chronic non-healing wounds and difficult-to-heal diabetic skin defects. At the same time, we initially explored the role of macrophages in assisting AFG treating diabetic wounds, and found that AFG can promote the infiltration of macrophages to promote the secretion of wound-healing related growth factors and revascularization, which is crucial for improving the wound-healing environment and ECM reconstruction.

Acknowledgments

Disclosure

The authors report no conflicts of interest in this work.

References

1. Fard AS, Esmaelzadeh M, Larijani B, Assessment and treatment of diabetic foot ulcer. *Int J Clin Pract*. 2007;61:1931–1938. doi:10.1111/j.1742-1241.2007.01534.x
2. Eming SA, Krieg T, Davidson JM. Inflammation in wound repair: molecular and cellular mechanisms. *J Invest Dermatol*. 2007;127:514–525. doi:10.1038/sj.jid.5700701
3. Werner S, Krieg T, Smola H. Keratinocyte-fibroblast interactions in wound healing. *J Invest Dermatol*. 2007;127:998–1008. doi:10.1038/sj.jid.5700786
4. Sen CK, et al. Human skin wounds: a major and snowballing threat to public health and the economy. *Wound Repair Regen*. 2009;17:763–771. doi:10.1111/j.1524-475X.2009.00543.x

5. Jiang X, et al. Limb salvage and prevention of ulcer recurrence in a chronic refractory diabetic foot osteomyelitis. *Diabetes Metab Syndr Obes*. 2020;13:2289–2296. doi:10.2147/DMSO.S254586
6. Yekta Z, et al. Clinical and behavioral factors associated with management outcome in hospitalized patients with diabetic foot ulcer. *Diabetes Metab Syndr Obes*. 2011;4:371–375. doi:10.2147/DMSO.S25309
7. Goodarzi P, et al. Tissue engineered skin substitutes. *Adv Exp Med Biol*. 2018;1107:143–188.
8. Debels H, et al. Dermal matrices and bioengineered skin substitutes: a critical review of current options. *Plast Reconstr Surg Glob Open*. 2015;3:e284. doi:10.1097/GOX.0000000000000219
9. Moura LI, et al. Recent advances on the development of wound dressings for diabetic foot ulcer treatment – a review. *Acta Biomater*. 2013;9:7093–7114. doi:10.1016/j.actbio.2013.03.033
10. Rosado P, et al. Influence of diabetes mellitus on postoperative complications and failure in head and neck free flap reconstruction: a systematic review and meta-analysis. *Head Neck*. 2015;37:615–618. doi:10.1002/hed.23624
11. Nicholas MN, Yeung. J. Current status and future of skin substitutes for chronic wound healing. *J Cutan Med Surg*. 2017;21:23–30. doi:10.1177/1203475416664037
12. Vileikyte L. Diabetic foot ulcers: a quality of life issue. *Diabetes Metab Res Rev*. 2001;17:246–249. doi:10.1002/dmrr.216
13. Conde-Green A, et al. Fat grafting and adipose-derived regenerative cells in burn wound healing and scarring: a systematic review of the literature. *Plast Reconstr Surg*. 2016;137:302–312. doi:10.1097/PRS.0000000000001918
14. Jackson WM, Nesti LJ, Tuan RS. Mesenchymal stem cell therapy for attenuation of scar formation during wound healing. *Stem Cell Res Ther*. 2012;3:20. doi:10.1186/scrt111
15. Nishiwaki K, et al. In situ transplantation of adipose tissue-derived stem cells organized on porous polymer nanosheets for murine skin defects. *J Biomed Mater Res B Appl Biomater*. 2019;107:1363–1371. doi:10.1002/jbm.b.34228
16. Chen YW, et al. The effects of adipose-derived stem cell-differentiated adipocytes on skin burn wound healing in rats. *J Burn Care Res*. 2017;38:1–10. doi:10.1097/BCR.0000000000000466
17. Trottier V, et al. IFATS collection: using human adipose-derived stem/stromal cells for the production of new skin substitutes. *Stem Cells*. 2008;26:2713–2723. doi:10.1634/stemcells.2008-0031
18. Zhou X, et al. Multiple injections of autologous adipose-derived stem cells accelerate the burn wound healing process and promote blood vessel regeneration in a rat model. *Stem Cells Dev*. 2019;28:1463–1472. doi:10.1089/scd.2019.0113
19. Frueh FS, et al. The crucial role of vascularization and lymphangiogenesis in skin reconstruction. *Eur Surg Res*. 2018;59:242–254. doi:10.1159/000492413
20. Moura J, et al. Molecular and cellular mechanisms of bone morphogenetic proteins and activins in the skin: potential benefits for wound healing. *Arch Dermatol Res*. 2013;305:557–569. doi:10.1007/s00403-013-1381-2
21. Fui LW, et al. Understanding the multifaceted mechanisms of diabetic wound healing and therapeutic application of stem cells conditioned medium in the healing process. *J Tissue Eng Regen Med*. 2019;13:2218–2233. doi:10.1002/term.2966
22. Naderi A, et al. Long term features of diabetic retinopathy in streptozotocin-induced diabetic Wistar rats. *Exp Eye Res*. 2019;184:213–220. doi:10.1016/j.exer.2019.04.025
23. Lee YJ, et al. Wound-healing effect of adipose stem cell-derived extracellular matrix sheet on full-thickness skin defect rat model: histological and immunohistochemical study. *Int Wound J*. 2019;16:286–296. doi:10.1111/iwj.13030
24. Kurita M, et al. Influences of centrifugation on cells and tissues in liposuction aspirates: optimized centrifugation for lipotransfer and cell isolation. *Plast Reconstr Surg*. 2008;121:1033–1041. doi:10.1097/01.prs.0000299384.53131.87

25. Opperman KS, et al. Clodronate-liposome mediated macrophage depletion abrogates multiple myeloma tumor establishment in vivo. *Neoplasia*. 2019;21:777–787. doi:10.1016/j.neo.2019.05.006

26. Xu J, et al. miRNA-221-3p in endothelial progenitor cell-derived exosomes accelerates skin wound healing in diabetic mice. *Diabetes Metab Syndr Obes*. 2020;13:1259–1270. doi:10.2147/DMSO.S243549

27. Zarei F, Negahdari B, Eatemadi A. Diabetic ulcer regeneration: stem cells, biomaterials, growth factors. *Artif Cells Nanomed Biotechnol*. 2018;46:26–32. doi:10.1080/21691401.2017.1304407

28. Qing C. The molecular biology in wound healing & non-healing wound. *Chin J Traumatol*. 2017;20:189–193. doi:10.1016/j.cjtee.2017.06.001

29. Arosi I, Hiner G, Rajbhandari S. Pathogenesis and treatment of callus in the diabetic foot. *Curr Diabetes Rev*. 2016;12:179–183. doi:10.2174/1573399811666150609160219

30. Hong P, et al. The functions and clinical application potential of exosomes derived from adipose mesenchymal stem cells: a comprehensive review. *Stem Cell Res Ther*. 2019;10:242.

31. Mazini L, et al. Regenerative capacity of adipose derived stem cells (ADSCs), comparison with mesenchymal stem cells (MSCs). *Int J Mol Sci*. 2019;20.

32. Hassan WU, Greiser U, Wang W. Role of adipose-derived stem cells in wound healing. *Wound Repair Regen*. 2014;22:313–325. doi:10.1111/wrr.12173

33. Rohrich RJ, Wan D. Making sense of stem cells and fat grafting in plastic surgery: the hype, evidence, and evolving U.S. Food and drug administration regulations. *Plast Reconstr Surg*. 2019;143:417e–424e. doi:10.1097/PRS.0000000000005207

34. Smith OJ, Jell G, Mosahebi A. The use of fat grafting and platelet-rich plasma for wound healing: a review of the current evidence. *Int Wound J*. 2019;16:275–285. doi:10.1111/iwj.13029

35. Quaglino DJ, et al. Transforming growth factor-beta stimulates wound healing and modulates extracellular matrix gene expression in pig skin: incisional wound model. *J Invest Dermatol*. 1991;97:34–42.

36. Werner S, Grose R. Regulation of wound healing by growth factors and cytokines. *Physiol Rev*. 2003;83:835–870. doi:10.1152/physrev.2003.83.3.835

37. Greenhalgh DG, et al. PDGF and FGF stimulate wound healing in the genetically diabetic mouse. *Am J Pathol*. 1990;136:1235–1246.

38. Li M, et al. Macrophage-derived exosomes accelerate wound healing through their anti-inflammation effects in a diabetic rat model. *Artif Cells Nanomed Biotechnol*. 2019;47:3793–3803. doi:10.1080/21691401.2019.1669617

39. Kim SY, Nair MG. Macrophages in wound healing: activation and plasticity. *Immunol Cell Biol*. 2019;97:258–267. doi:10.1111/imcb.12236

40. Karimi H, et al. Burn wound healing with injection of adipose-derived stem cells: a mouse model study. *Ann Burns Fire Disasters*. 2014;27:44–49.

41. Ricard-Blum S, Baffet G, Theret N. Molecular and tissue alterations of collagens in fibrosis. *Matrix Biol*. 2018;68–69:122–149. doi:10.1016/j.matbio.2018.02.004

42. Goffin JM, et al. Focal adhesion size controls tension-dependent recruitment of alpha-smooth muscle actin to stress fibers. *J Cell Biol*. 2006;172:259–268. doi:10.1083/jcb.200506179

43. Follonier CL, et al. Regulation of myofibroblast activities: calcium pulls some strings behind the scene. *Exp Cell Res*. 2010;316:2390–2401. doi:10.1016/j.yexcr.2010.04.033